Decoherence and dissipation during a quantum XOR gate operation

Michael Thorwart
Institut für Physik, Universität Augsburg, Universitätsstraße 1, 86135 Augsburg, Germany
and Department of Applied Physics, Delft University of Technology, Lorentzweg 1, 2628 CJ Delft, The Netherlands

Peter Hänggi
Institut für Physik, Universität Augsburg, Universitätsstraße 1, 86135 Augsburg, Germany
(Received 26 April 2001; published 11 December 2001)

The dynamics of a generic quantum XOR gate operation involving two interacting qubits being coupled to a bath of quantum harmonic oscillators is explored. By use of the formally exact quasiadiabatic-propagator path-integral methodology we study the time-resolved evolution of this interacting and decohering two-qubit system in presence of time-dependent external fields. The quality of the XOR gate operation is monitored by evaluating the four characteristic gate quantifiers: fidelity, purity, the quantum degree, and the entanglement capability of the gate. Two different types of errors for the XOR operation have been modeled, i.e., (i) bit-flip errors and (ii) phase errors. The various quantifiers are systematically investigated vs the strength of the *interqubit coupling* and vs both, the environmental *temperature* and the (Ohmic-like) *bath-interaction strength.* Our main findings are that these four gate quantifiers depend only very *weakly* on temperature, but are *extremely sensitive* to the bath-interaction strength. Interestingly enough, however, we find that the XOR gate operation deteriorates only weakly upon decreasing the interqubit coupling strength. This generic case study yields lower bounds on the quality of realistic XOR gate operations.

DOI: 10.1103/PhysRevA.65.012309 PACS number(s): 03.67.Lx, 03.65.Yz, 89.70.+c, 05.30.−d

I. INTRODUCTION

The basic elements of quantum computation are logic quantum gates, which represent manipulations of quantum bits, $|0\rangle$ and $|1\rangle$, according to Boolean algebra. Any arbitrary complex logic operation can be build up of only a few basic gates (*universal gates*) [1] and one can show that almost every gate that operates on two or more qubits is a universal gate [2]. The explicit construction of quantum networks for elementary arithmetic operations then becomes possible upon appropriately combining such universal gates; see, for instance, Ref. [3] for the explicit construction of the addition or the modular exponentiation. In turn, this permits the implementation of Shor's quantum factorizing algorithm [4] in terms of elementary gates. Together with Deutsch's algorithm [5], these two quantum algorithms are presently the most important examples that are known to be superior to their classical counterparts and which do justify the current efforts towards a technological realization of a quantum computer.

In this work we concentrate on one such elementary gate, namely, the *quantum exclusive OR* (*XOR*) gate. It is a unitary transformation that propagates an initial state $|\Psi_{\rm in}\rangle$ of a two-qubit system to a final state $|\Psi_{\rm out}\rangle = U_{\rm XOR}|\Psi_{\rm in}\rangle$. Represented in the computational basis $|b_i\rangle \in \{|00\rangle, |01\rangle, |10\rangle, |11\rangle\}$ ($i = 1, \ldots, 4$), the XOR gate operation can be written as

$$U_{\rm XOR} = \begin{pmatrix} 1 & 0 & 0 & 0 \\ 0 & 1 & 0 & 0 \\ 0 & 0 & 0 & 1 \\ 0 & 0 & 1 & 0 \end{pmatrix}. \tag{1.1}$$

Since this operation inverts the state of the second qubit of the basis states if the first qubit is in the state $|1\rangle$, this operation is also called the *quantum controlled-NOT* (*CNOT*) gate. The set of all one-qubit gates together with the quantum XOR gate is universal, as has been demonstrated in Ref. [6].

The main impediment on the roadway to a working quantum computer is decoherence [7–12]. It disturbs the phase relation in a quantum superposition state and therefore is effective at the roots where the quantum computer is believed to have its most important advantage. Any realistic quantum computer will have some interaction with its environment, which induces decoherence (decay of the off-diagonal elements of the reduced density matrix) and dissipation (change of populations of the reduced density matrix). Moreover, other sources for decoherence that are due to imperfect gate operations and cross talks of the qubits within a register need to be considered [10].

Several previous works in the literature deal with the effect of decoherence in quantum information processing systems. Unruh [7] and Palma *et al.* [9] consider a model of a single qubit, which is represented by the eigenstates of the quasispin operator σ_z and which couples to a bosonic environment via its σ_z component. It describes appropriately the dephasing (decoherence) but does not include population exchange (dissipation). Combining L *noninteracting* qubits of this type, they estimate the decoherence (in the limit of a large coherence length of the bath) to increase exponentially with the length L of the register.

Dissipative effects (bit-flip errors) are properly described by the so-called spin-boson model [13–16], where the qubit is represented by the σ_x component of the spin 1/2, but the coupling to the bosonic bath is mediated by the σ_z component of the spin-1/2 (note that this refers to the localized representation). In this model, the bath also induces transitions between the two system eigenstates (bit flips) and—in

addition to decoherence—energy is exchanged between system and bath. The general solution of the problem in terms of a generalized (non-Markovian) master equation for the entire reduced density matrix for an arbitrary initial preparation in the presence of a static bias and also for a time-dependent driving has been given in Ref. [16]. In our work, the assumption of a Markovian bath and of a weak system-bath interaction (Bloch-Redfield approach), which may restrict the validity of the master equation (see below), is not made.

The previously discussed works concern the investigation of decoherence in single qubits or in a register of noninteracting qubits. Decoherence and dissipation in a system of *interacting* qubits has been studied only rarely. The dynamics of two coupled two-level systems has been investigated by Dubé and Stamp [17] by means of a general model for coupled Josephson junctions, for coupled nanomagnets, or for interacting Kondo impurities. Each two-level system is represented (in the tunneling representation) by the σ_x component of a spin 1/2. The two spins interact via their σ_z components. Moreover, their σ_z components couple to a bosonic bath. By use of real-time path integrals the dynamics of the relaxation process is determined. Although no specific problem of quantum information processing is investigated, this is the first work where two interacting spins in a dissipative bath have been considered.

A similar model has been studied by Governale, Grifoni, and Schön [18]. Two biased spin-(1/2) systems interact via their σ_y components, which is the appropriate coupling for Josephson-junction charge qubits (see below). Moreover, their σ_z components couple either to the same or to different bosonic baths. Applying the widely used Bloch-Redfield formalism, the time evolution of the populations of the logical states is evaluated. This model describes dissipation being caused by fluctuations in voltage sources in Josephson-junction charge qubits (see below). However, no specific quantum-information operation has been considered.

A two-qubit quantum gate for quantum information processing in coupled quantum dots has been investigated in Refs. [11,19]. Two spin-(1/2) systems are coupled using a time-dependent Heisenberg-type interaction. Moreover, a coupling of the spins to a bosonic bath has been taken into account. By solving the quantum Liouville equation in the limit of weak system-bath coupling (Born-Markov approximation) for the reduced density operator, the purity and the fidelity of the swap operation $U_{\mathrm{swap}}|ij\rangle=|ji\rangle$ $(i,j=0,1)$ is calculated as a function of time. However, the authors consider the time evolution of the quantum system *after the swap operation has been completed*. The same is true for the XOR gate operation in Ref. [11], where, additionally, a further assumption has been made: The pulse sequence to realize the quantum XOR consists of four pulses of the external fields. Each pulse is taken to be constant over the corresponding time interval. To obtain the solution over the entire time span within the Born-Markov approximation, it is necessary to assume a finite time interval between the single pulses. This is required because the Born-Markov approximation is known to violate positivity of the reduced density operator at short transient times [20,21]. This additional time span (pulse-to-pulse time) has been taken as three times the switching time interval. This leads to an extension of the computation time, which is only due to formal mathematical reasons and which deteriorates the quality of the gate operation. Moreover, a systematic study of the dependence of the gate quantifiers on the relevant parameters has not been given.

In this work, we investigate systematically the XOR quantum gate in presence of an interaction of the qubits with their environment. Thereby, we take into account the full time dependence of the external fields, which induce the XOR operation without invoking further approximations on the system Hamiltonian. In particular, we use the numerical *ab initio* technique of the quasiadiabtic-propagator path integral (QUAPI) [22] (for other applications, see also Refs. [23,24]). This numerically precise iterative real-time path-integral method does not suffer from the above-mentioned problem of lacking positivity. In order to realize the logic XOR operation in physical systems, we introduce a generic model Hamiltonian, which is suitable for studying the XOR operation on a very general and idealized level. We determine the quality of the gate by calculating the four characteristic gate quantifiers introduced by Poyatos, Cirac, and Zoller [25]; namely, the (i) purity, (ii) fidelity, (iii) quantum degree, and (iv) entanglement capability. To that end, we consider two important types of computational errors, i.e., phase errors and bit-flip errors. The former can be modeled by coupling the σ_z component of each spin to the bath while the later is induced by coupling the σ_x component of each spin to the bath. We are mainly interested in the quality of the gate operation during its time evolution and, most importantly, right after it has been completed. We choose three different parameter sets for which different coupling constants in the qubit Hamiltonian lead to differently long time intervals required for the gate operation.

So far, we have discussed theoretical aspects of quantum information processing. However, those refined and highly elaborate concepts face the question of how they can be implemented in experimental hardware. Several proposals to build a quantum information processor exist. Prominent candidates are, for instance, atoms in optical cavities, ions in linear or Paul traps interacting with laser beams, or nuclear spins in a nuclear magnetic resonance liquid [26]. Although the experimental techniques in those fields of research are currently most advanced, the problem of upscaling of a quantum computer can seemingly only be solved within condensed-matter systems that can be embeded in an electronic circuit. Promiment systems for condensed-matter qubits are flux states of a SQUID (superconducting quantum interference device) (*flux qubits*) [27] (see also [12]), charge states of superconducting islands with Josephson junctions (*charge qubits*) [12,28], and spin [11,29] or charge [30] states in ultrasmall coupled semiconductor quantum dots (*quantum-dot qubits*). Moreover, several realizations of qubits in nuclear [31,32] and electronic [32,33] spins in semiconductor nanostructures have been proposed.

The paper is organized as follows: In Sec. II, we introduce a generic model as a starting point for the quantum XOR operation including the interaction with the environment. In Sec. III, we present a brief review on the numerical tech-

nique of the QUAPI, which we employ in the following. In order to determine the quality of the decoherent XOR gate, we use four quantifiers which are introduced in Sec. IV. The results and the conclusions are presented in Secs. V and VI, respectively.

II. A GENERIC MODEL FOR THE QUANTUM XOR GATE

A. The coherent XOR operation

The quantum XOR gate is a two-qubit operation that can be modeled by two coupled spin-(1/2) systems represented by the Pauli operators $\vec{\sigma}_j=(\sigma_j^x,\sigma_j^y,\sigma_j^z)^T$, $j=1,2$. The two logical states of each qubit are represented by the two eigenstates of the σ_z component of each spin, i.e., $|0\rangle_j\equiv|\uparrow\rangle_j$ and $|1\rangle_j\equiv|\downarrow\rangle_j$. We assume that the single qubit as well as the coupling between the two qubits can be controlled by switching on (local) external fields, for instance, magnetic fields. This system can generically be described [12] by the generic Hamiltonian

$$H_{\mathrm{XOR}}(t)=-\frac{\hbar}{2}\sum_{j=1}^{2}\vec{B}_j(t)\vec{\sigma}_j+\hbar\sum_{j\neq k}J(t)\sigma_j^+\sigma_k^-, \quad (2.1)$$

where $\sigma_j^{\pm}=(\sigma_j^x\pm i\sigma_j^y)/2$. Moreover, $\vec{B}_j(t)=(B_j^x(t),0,B_j^z(t))^T$, $j=1,2$ are time-dependent coupling strengths (with the dimension of a frequency) arising from local time-dependent external fields at the site of the spin j in longitudinal (z) or transverse (x) direction. In Eq. (2.1), the coupling between the two qubits is assumed to be symmetric; furthermore, it should be controllable from the outside leading to a time-dependent interaction strength $J(t)$. The particular form of the interaction in Eq. (2.1) is only one example. We note that this generic model does not account for the particular details of a physical realization of qubits in a specific condensed-matter system. For each individual system, such as flux qubits or charge qubits, the Hamiltonian looks different in detail. In particular, the coupling term between the two qubits takes different forms. However, all two-qubit Hamiltonians have a structure that is similar to our generic model in Eq. (2.1). The general physical behavior will be similar such that our generic model serves as an archetype.

The quantum XOR gate (1.1) can be obtained by a sequence of one- and two-qubit operations according to [12]

$$U_{\mathrm{XOR}}=U_2^x\left(\frac{\pi}{2}\right)U_2^z\left(-\frac{\pi}{2}\right)U_2^x(-\pi)U_{12}\left(-\frac{\pi}{2}\right)U_1^x\left(-\frac{\pi}{2}\right)$$
$$\times U_{12}\left(\frac{\pi}{2}\right)U_1^z\left(-\frac{\pi}{2}\right)U_2^z\left(-\frac{\pi}{2}\right), \quad (2.2)$$

where

$$U_j^{x/z}(\alpha)=\exp\left(i\frac{\alpha}{2}\sigma_j^{x/z}\right), \quad j=1,2,$$

$$U_{12}(\beta)=\exp[i\beta(\sigma_1^+\sigma_2^-+\sigma_1^-\sigma_2^+)] \quad (2.3)$$

are the propagators over the single time intervals with the external fields in the Hamiltonian, Eq. (2.1), switched on and off in the following way: In order to attain this propagator, a pulse sequence of the external fields is necessary. For simplicity we assume throughout this work, that the pulses are switched instantaneously on and off and are constant over the time span $t_{\mathrm{off}}-t_{\mathrm{on}}$ during which they are on. This induces time-dependent interaction strengths $\mathcal{B}(t)=\mathcal{B}[\Theta(t-t_{\mathrm{on}})-\Theta(t-t_{\mathrm{off}})]$ with $\mathcal{B}=B_j^{(x/z)}$, $J=\mathrm{const}$ and with $\Theta(t)$ being the Heaviside function. Furthermore, we assume that both spins are equal and experience local fields of equal strength. This implies $B_1^{x/z}=B_2^{x/z}\equiv B^{x/z}$. The angles α and β in Eq. (2.3) are related to the actual physical propagation time t according to

$$\alpha=B^{x/z}t \quad \text{and} \quad \beta=Jt. \quad (2.4)$$

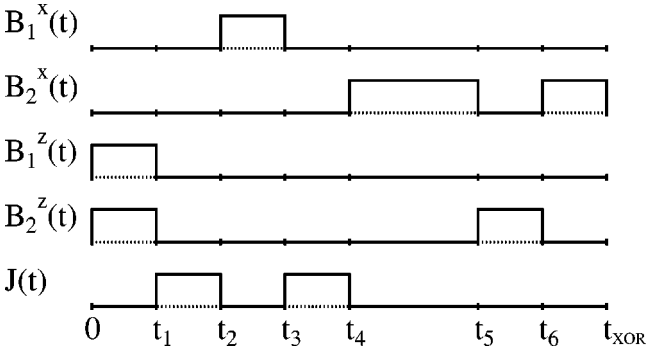

FIG. 1. Schematic view of a pulse sequence necessary to generate the quantum XOR gate. The parameters are set to $B^x=B^z=J=\mathrm{const}$. The frequencies are given in units of B^z while the time is scaled in units of $(B^z)^{-1}$. The switching times t_j are given in the text and are in this case equal to multiples of $\pi/2$.

The switching times then follow as $t_1=\pi/(2B^z)$, $t_2=t_1+\pi/(2J)$, $t_3=t_2+\pi/(2B^x)$, $t_4=t_3+\pi/(2J)$, $t_5=t_4+\pi/(B^x)$, $t_6=t_5+\pi/(2B^z)$, and $t_{\mathrm{XOR}}=t_6+\pi/(2B^x)$, where t_{XOR} denotes the total time elapsed during the full XOR gate operation. An example of this pulse sequence is sketched in Fig. 1 for the case of $B^x=B^z=J$. The coupling constants are given in units of B^z while the time is scaled in units of $(B^z)^{-1}$. One immediately observes that the computation time t_{XOR} is extended if the coupling energies are decreased. We note that the assumption of rectangular pulses is not required by the numerical technique we use and is made here only for the sake of simplicity. We could also consider other shapes of the pulses that are more realistic for specific physical systems, and especially, we could consider imperfect switching processes as well; the latter would constitute a further source of decoherence. In this respect, our generic model is minimal since it assumes precise control over the deterministic part of the time evolution via precise control of the external fields. More realistic assumptions on the external driving fields like nonrectangular pulse shapes or imperfect switching would deteriorate our findings as these effects are an additional source of decoherence.

B. Interaction with the environment

We model the interaction of the qubit system with the fluctuating environment by a Hamiltonian, in which $H_{\rm XOR}(t)$ is coupled to a bath of harmonic oscillators, i.e.,

$$H(t)=H_{\rm XOR}(t)+H_B+H_{\rm int}^{x/z} \tag{2.5}$$

with

$$H_B=\sum_{j=1}^{N}\hbar\omega_j\left(a_j^\dagger a_j+\frac{1}{2}\right). \tag{2.6}$$

Here, $a_j^\dagger$ (a_j) denotes the creation (annihilation) operator of the jth bath oscillator with frequency ω_j. Since we want to investigate the role of bit-flip errors as well as phase errors we include in our model two different types of interactions. On the one hand, the σ^x components of the spins couple to the fluctuating environment and the populations of the qubit states are disturbed (bit-flip errors). On the other hand, phase errors are generated by coupling of the σ^z components of the spins to the environmental noise. This is conveniently modeled by the form

$$H_{\rm int}^{x/z}=\frac{\hbar}{2}(\sigma_1^{x/z}+\sigma_2^{x/z})\sum_{j=1}^{N}\kappa_j^{x/z}(a_j^+ +a_j), \tag{2.7}$$

where $\kappa_j^{x/z}$ denotes the coupling strength of the jth oscillator to the system and where the superscript (x/z) denotes *one or the other kind of interaction*. We note that we assume here a coupling of the two spins to the same bath. This implies that the spins are effectively coupled to each other via the bath. A coupling of the spins to different (uncorrelated) baths could be readily incorporated in the numerical QUAPI technique (see below).

To study the dynamics of this system, we have to specify the initial conditions. Throughout this work, we assume that the density operator $W(t)$ of the entire system plus bath at initial time $t=0$ factorizes according to

$$W(0)=\rho_{\rm S}(0)\otimes\rho_B. \tag{2.8}$$

$\rho_{\rm S}(0)$ is the density operator of the system at time $t=0$ and $\rho_B=Z_B^{-1}\exp[-H_B/(k_BT)]$ is the canonical equilibrium distribution of the (decoupled) bath at temperature T. Moreover, $Z_B=\mathrm{tr}\exp[-H_B/(k_BT)]$ and k_B denotes the Boltzmann constant.

The influence of the bath is fully characterized [14] by the spectral density

$$\Gamma^{x/z}(\omega)=2\pi\sum_{j=1}^{N}(\kappa_j^{x/z})^2\delta(\omega-\omega_j), \tag{2.9}$$

which assumes a continuous form if the number N of oscillators approaches infinity. Throughout this work, we apply an Ohmic spectral density with an exponential cutoff, i.e.,

$$\Gamma^{x/z}(\omega)=\gamma^{x/z}\omega\exp(-\omega/\omega_c), \tag{2.10}$$

where the dimensionless bath-interaction constant $\gamma^{x/z}$ characterizes the strength of the interaction with the environment. This spectrum mimics the environmentally induced fluctuations in the external circuit, which supplies flux through the SQUID loops in the flux qubits [12,27]. Moreover, background-charge fluctuations in the voltage sources in Josephson charge qubits [12,28] also lead to an Ohmic impedance R. Similarly, electronic states in coupled quantum-dot qubits experience an Ohmic environment, either for the spin [11,29] or for the charge [30] degrees of freedom.

III. NUMERICAL *AB INITIO* TECHNIQUE: QUAPI

In order to describe the dynamics of the two-qubit system of interest it is sufficient to consider the time evolution of the reduced density operator

$$\rho(t)=\mathrm{tr}_{\rm bath}\,\mathcal{U}(t,0)W(0)\mathcal{U}^{-1}(t,0),$$

$$\mathcal{U}(t,0)=\mathcal{T}\exp\left\{-i/\hbar\int_0^t H(t')dt'\right\}. \tag{3.1}$$

Here, $\mathcal{U}(t,0)$ is the propagator of the full system plus bath and $\mathcal{T}$ denotes the time-ordering operator. Moreover, $\mathrm{tr}_{\rm bath}$ means the partial trace over the harmonic bath oscillators. Due to our assumption that the bath is initially at thermal equilibrium and decoupled from the system, see Eq. (2.8), the partial trace over the bath can be performed. We denote the matrix elements of the reduced density matrix in the computational basis with $\rho_{ij}(t)\equiv\langle b_i|\rho(t)|b_j\rangle$ and rewrite them according to Feynman and Vernon [34] as

$$\rho_{ij}(t)=\sum_{m,n=1}^{4}G_{ij,mn}(t,0)\rho_{mn}(0), \tag{3.2}$$

with the propagator G given by

$$G_{ij,mn}(t,0)=\int\mathcal{D}x\mathcal{D}x'\mathcal{A}[x]\mathcal{A}^*[x']\mathcal{F}_{\rm FV}[x,x']. \tag{3.3}$$

The functional $\mathcal{A}[x]$ denotes the probability amplitude for the free system to follow the path $x(t)$ and $\mathcal{F}_{\rm FV}[x,x']$ denotes the Feynman-Vernon influence functional [34] (see Ref. [14] for details). The functional integrations in Eq. (3.3) extend over paths with end points $x(0)=x_m$, $x(t)=x_i$, $x'(0)=x_n$, and $x'(t)=x_j$, which belong to the initial and final states, $\rho_{mn}(0)$ and $\rho_{ij}(t)$, respectively.

The technique that we use to calculate the reduced density operator, Eq. (3.2), is the iterative tensor multiplication scheme derived for the so-called QUAPI. This numerical algorithm was developed by Makri and Makarov [22] within the context of chemical physics. Since its first applications it has been succesfully tested and adopted to various problems of open quantum systems, with and without external driving [22–24]. Because the details of this algorithm have been extensively discussed previously in the literature [22–24], we only mention those prominent ingredients that are of importance for our work.

(i) Symmetric splitting of the short-time propagator: To obtain a numerical iteration scheme, we discretize the time interval $[0,t]$ into $\mathcal{N}$ steps Δt, such that $t_k = k\Delta t$ and split symmetrically the full propagator over one time step $\mathcal{U}(t_{k+1},t_k)$ in Eq. (3.1), according to the Trotter formula, into a system and an environmental part,

$$\mathcal{U}(t_{k+1},t_k) \approx \exp(-iH_B\Delta t/2\hbar)\mathcal{U}_S(t_{k+1},t_k) \times \exp(-iH_B\Delta t/2\hbar),$$

$$\mathcal{U}_S(t_{k+1},t_k) = \mathcal{T}\exp\left\{-\frac{i}{\hbar}\int_{t_k}^{t_{k+1}} dt' H_{\mathrm{XOR}}(t')\right\}. \quad (3.4)$$

The neglect of higher-order terms of the propagator in Eq. (3.4) causes an error of the order of Δt^3. The short-time propagator $\mathcal{U}_S$ of the bare system is given by the corresponding exact system propagators in Eq. (2.3) over a time step Δt. At this point, we emphasize that this method is not plagued by the problem of lacking positivity of the density operator at short times, as is the case for the usually employed master-equation approach in the Born-Markov limit [11,19]. The *exact* coherent dynamics of the bare system enters and the decomposition of the short-time propagator according to Eq. (3.4) is valid for any arbitrary short time.

(ii) The interaction with the bath induces correlations among the paths (memory) that are described by the influence functional in Eq. (3.3). As long as the temperature of the Ohmic bath is finite, these correlations decay exponentially fast with increasing time [14]. This motivates to neglect such long-time correlations and to break up the influence kernels into smaller pieces of length $K\Delta t$, where K denotes the number of time steps over which the memory is fully taken into account.

The two strategies in (i) and (ii) are countercurrent. In step (i) a small time step Δt is desirable in order to minimize the error due to the neglected higher-order terms in the propagator. On the other hand, in (ii) a large time step is needed in order to take a long memory range into account. A compromise between those two errors has to be found in practice by applying the principle of minimal sensitivity [24] to adjust the two parameters Δt and K, see discussion below.

(iii) The third important ingredient is the appropriate choice of basis representation of the problem. For the algorithm it is required to iterate the dynamics in the eigenbasis of that system operator, which couples to the bath. Then the influence functional in Eq. (3.3) can be evaluated in terms of the eigenvalues of the coupling operator. In problems where the coordinate of a quantum particle in a continuous potential is damped, the continuous position operator turns into a discrete set of position eigenvalues. Hence, this representation has been termed the *discrete variable representation*.

Bit-flip errors. If the σ_x components of each spin couple to the bath, see Eq. (2.7), the eigenbasis of the coupling operator is determined by $\langle\alpha_i|(\sigma_1^x+\sigma_2^x)/2|\alpha_j\rangle = \lambda_i\,\delta_{ij}$ with $\lambda_1=0$, $\lambda_2=-1$, $\lambda_3=1$, and $\lambda_4=0$. A basis rotation of the computational basis with basis states $|b_j\rangle$ has to be performed according to

$$|\alpha_i\rangle = \sum_{j=1}^{4} R_{ij}|b_j\rangle, \quad (3.5)$$

with the transformation matrix

$$R = \frac{1}{2}\begin{pmatrix} 1 & 1 & 1 & -1 \\ -1 & -1 & 1 & -1 \\ 1 & -1 & 1 & 1 \\ -1 & 1 & 1 & 1 \end{pmatrix}. \quad (3.6)$$

Phase errors. For the second case that the σ_z components of each spin couple to the bath in Eq. (2.7), the system part of Hamiltonian is already diagonal in the computational basis, i.e., $\langle b_i|(\sigma_1^z+\sigma_2^z)/2|b_j\rangle = \lambda_i\delta_{ij}$ with $\lambda_1=1$, $\lambda_2=0$, $\lambda_3=0$, and $\lambda_4=-1$. No additional basis transformation is necessary.

IV. CHARACTERISTIC GATE QUANTIFIERS

In order to quantify the *quality* of the quantum gate, we use four global parameters that have been defined by Poyatos, Cirac, and Zoller [25]: (i) the gate fidelity $\mathcal{F}$, (ii) the gate purity $\mathcal{P}$,(iii) the quantum degree $\mathcal{Q}$ of the gate, and (iv) the entanglement capability $\mathcal{C}$ of the gate. These four quantifiers can be calculated once the reduced density operator ρ in Eq. (3.1) is determined. To this end, 16 unentangled input states $|\Psi_{\mathrm{in}}^j\rangle$, $j=1,\ldots,16$ are defined according to $|\psi_a\rangle_1|\psi_b\rangle_2$ $(a,b=1,\ldots,4)$, with $|\psi_1\rangle=|0\rangle$, $|\psi_2\rangle=|1\rangle$, $|\psi_3\rangle=(|0\rangle+|1\rangle)/\sqrt{2}$, and $|\psi_4\rangle=(|0\rangle+i|1\rangle)/\sqrt{2}$. They form one possible basis set and span the Hilbert space for the superoperator $\mathcal{V}_{\mathrm{XOR}}$, where $\rho(t_{\mathrm{XOR}})=\mathcal{V}_{\mathrm{XOR}}\rho(0)$, see Ref. [25] for details. Moreover, these basis states are chosen to be unentangled states in order to avoid the application of a preceding two-qubit gate for the preparation of the system state.

The gate fidelity $\mathcal{F}$ is defined as the overlap between the propagation with the ideal propagator U_{XOR}, Eq. (1.1), averaged over all 16 initial states $|\Psi_{\mathrm{in}}^j\rangle$ according to

$$\mathcal{F} = \frac{1}{16}\sum_{j=1}^{16}\langle\Psi_{\mathrm{in}}^j|U_{\mathrm{XOR}}^{+}\rho_{\mathrm{XOR}}^j U_{\mathrm{XOR}}|\Psi_{\mathrm{in}}^j\rangle \quad (4.1)$$

with $\rho_{\mathrm{XOR}}^j=\rho(t_{\mathrm{XOR}})$, with initial condition $\rho(0)=|\Psi_{\mathrm{in}}^j\rangle\langle\Psi_{\mathrm{in}}^j|$.

In a similar way, the purity $\mathcal{P}$ is defined as

$$\mathcal{P} = \frac{1}{16}\sum_{j=1}^{16}\mathrm{tr}(\rho_{\mathrm{XOR}}^j)^2. \quad (4.2)$$

This quantity is proportional to the (negative) linearized entropy and reflects the effects of decoherence.

The third quantity, the quantum degree $\mathcal{Q}$ of the gate, is defined as the maximum of the overlap of all possible output states stemming from unentangled states and of all maximally entangled (Bell) states $|\Psi_{\mathrm{me}}^k\rangle$, $k=1,\ldots,4$. In formal terms, this implies

$$\mathcal{Q}=\max_{j,k}\langle\Psi^k_{\rm me}|\rho^j_{\rm XOR}|\Psi^k_{\rm me}\rangle. \tag{4.3}$$

The purpose of this parameter is to quantify the notion of nonlocality. Bennett and co-workers [35] have shown that all those density operators that have an overlap with a maximally entangled state being larger than the value $(2+3\sqrt{2})/8\approx 0.78$ are nonlocal, i.e., violate the Clauser-Horne-Shimony-Holt inequality [35].

Obviously, $\mathcal{F}=1$, $\mathcal{P}=1$, $\mathcal{Q}=1$ denote the ideal gate operation.

The fourth quantifier is the entanglement capability $\mathcal{C}$ of the gate. It denotes the smallest eigenvalue of the partial transposed density matrix [36], which is determined from $\rho^j_{\rm XOR}$ for all unentangled input states $|\Psi^j_{\rm in}\rangle$. $\rho^j_{\rm XOR}$ characterizes an entangled state if and only if the smallest eigenvalue of the partial transposed density operator is negative. The ideal operation has an entanglement capability of $\mathcal{C}=-0.5$.

V. RESULTS

Having determined the reduced matrix in Eq. (3.1) by the iterative QUAPI algorithm, we investigate the influence of the interaction with the environment systematically. Therefore, we assume that the two qubits are identical and experience external fields of the same strength, i.e., $B^x_1=B^x_2=B^x$ and $B^z_1=B^z_2=B^z$. Moreover, we introduce the following dimensionless parameters: We scale the quantities with respect to the characteristic energy scale of the single qubit, which is given by the energy splitting $\hbar B^z$ of the single qubit. This in turn defines a time scale $(B^z)^{-1}$. Consequently, the temperature is given in units of $\hbar B^z/k_B$ (Note that $\gamma^{x/z}$ is already dimensionless). For all following results, we have used a cutoff frequency of $\omega_c=50B^z$ in Eq. (2.10).

A. Time-resolved quantum XOR operation

We first illustrate the time-resolved dynamics of a generic XOR operation. To this end, we determine the populations of the four states of the computational basis as a function of time, i.e., $P_{ij}(t):=\langle ij|\rho(t)|ij\rangle$ with $i,j=0,1$ for the initial condition $\rho(0)=|11\rangle\langle 11|$. We choose the pulse sequence sketched in Fig. 1 with parameters $B^x=B^z$ and $J=B^z$. Moreover, we choose for illustrative purpose a rather high temperature of $T=0.1\hbar B^z/k_B$. Figure 2 depicts the results for the three different cases of (i) no coupling to the bath, $\gamma^{x/z}=0$ (solid line), (ii) bit-flip errors with $\gamma^x=0.01$ (long dashed line), and (iii) phase errors with $\gamma^z=0.01$ (dotted line). The switching times t_j are equal to multiples of $\pi/2$ for this special case of equal energies.

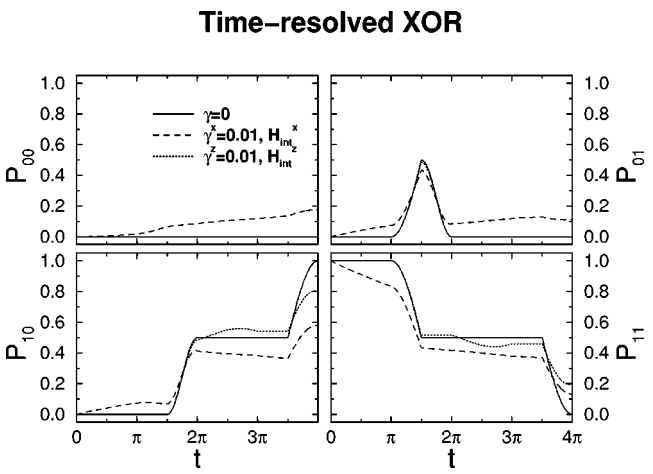

FIG. 2. Time-resolved dynamics of the quantum XOR operation for the case of equal energies, i.e., $B^x=B^z=J$. Depicted are the populations $P_{ij}(t)=\langle ij|\rho(t)|ij\rangle$ as a function of time for the initial condition $\rho(0)=|11\rangle\langle 11|$ for three different cases of (i) no coupling to the bath, $\gamma^{x/z}=0$ (solid line), (ii) bit-flip errors with $\gamma^x=0.01$ (long dashed line), and (iii) phase errors with $\gamma^z=0.01$ (dotted line). The time is scaled in units of $(B^z)^{-1}$. Moreover, we set the temperature to $T=0.1\hbar B^z/k_B$ and the cutoff frequency to $\omega_c=50B^z$.

The iterative QUAPI algorithm possesses two free parameters that have to be properly adjusted. We fix the number K of memory time steps and the length Δt of each time step according to the *principle of minimal sensitivity* [24]. By applying this method, we obtain the values $\Delta t=0.15(B^z)^{-1}$ with $K=2$ (not shown).

As one observes, the final state of the ideal operation $(\gamma^{x/z}=0)$ is $|\Psi\rangle=|10\rangle$. The deviation of the dynamics in presence of decoherence and dissipation from the ideal case is clearly visible.

We emphasize here that no additional time intervals between the switching events have been inserted as it would have been necessary for the application of Bloch-Redfield-type master-equation techniques.

B. Quality of different quantum XOR operations

In order to fix the parameter sets for the numerical simulations in the following investigations, we are guided by three different physical realizations of condensed-matter qu-

TABLE I. Parameter sets that have been used for the simulations of the quantum XOR gate. They mimic typical experimental situations for coupled qubit systems. The explcit values for three important solid-state qubit systems, i.e., flux qubits and charge qubits in superconducting Josephson devices (sets I and II) and spin and charge qubits in ultrasmall semiconductor quantum dots (set III) have been taken from literature (see text). The dimensionless time $t_{\rm XOR}B^z$ the entire gate operation takes is given in the last column.

Set	B^z	B^x	J	T	B^x/B^z	J/B^z	T/B^z	$t_{\rm XOR}B^z$
I (Flux qubits)	0.5 K	50 mK	25 mK	25 mK	0.1	0.05	0.05	$82(\pi/2)$
II (Charge qubits)	1 K	100 mK	5 mK	50 mK	0.1	0.005	0.05	$442(\pi/2)$
III (Quantum-dot qubits)	1 meV	1 meV	0.05 meV	125 mK	1	0.05	0.01	$46(\pi/2)$

bits, namely, flux qubits (set I) [27,12], charge qubits (set II) [12,28], and qubits realized in coupled semiconductor quantum dots (set III) [11,29].

The typical situation in superconducting qubits (set I and set II) is that the energy B^x for the σ^x components is one order of magnitude smaller than the characteristic energy B^z of the single qubits. The typical temperature in both cases is $T=0.05B^z$, while the interqubit coupling strength J for the charge qubits is one order of magnitude smaller than for the flux qubit. Hence the gate operation for set II takes longer than for set I and one would expect set II to be more exposed to decoherence. Therefore, set I should yield better results than set II. However, as we shall see below, this depends strongly on the kind of error induced by the bath, i.e., bit-flip or phase error.

In order to reduce the duration of the gate operation in comparison to set I, we choose $B^x=B^z$ in a third parameter set (set III). This choice implies that for set III the XOR takes the least time. Moreover, we additionally reduce temperature to $T=0.01B^z$ compared to set I. The third parameter set mimics typical experimental situations for coupled semiconductor quantum bits. The parameter sets are summarized in Table I. The total operation time t_{XOR} can easily be determined, see discussion below Eq. (2.4).

The QUAPI parameters are determined by the principle of minimal sensitivity for $K=3$. We obtain for the case of H^x_{int} (bit flip errors) for set I [in units of $(B^z)^{-1}$] $\Delta t=0.06$, for set II $\Delta t=0.2$, and for set III $\Delta t=0.02$, and for the case of H^z_{int} (phase errors) for set I $\Delta t=0.013$, for set II $\Delta t=0.08$, and for set III $\Delta t=0.01$.

1. Dependence on temperature

The dependence of the four characteristic gate quantifiers on the bath temperature T is depicted with Fig. 3. In panel (a) the influence of the random bit flips are investigated while panel (b) depicts the effect of phase errors. The bath-interaction constant for the bit-flip errors is chosen to be $\gamma^x=10^{-6}$ and for the phase errors we set $\gamma^z=10^{-4}$ [12].

First, one observes that all results depend only *very weakly* on temperature. Extrapolating the results to zero temperature indicates the influence of the nonvanishing quantum fluctuations of absolute zero. This behavior is typical for nonseparable quantum systems being bilinearly coupled to a harmonic bath [37]. Note that even at zero temperature finite damping is present because we do not monitor the (unitary) time evolution of the total system plus bath, but rather that of the physical subsystem being in contact with the bath. The environmental degrees of freedom, which are all traced out, are thus causing dissipation on the relevant system variables. At zero temperature, the second moment (and even-order higher ones) of the quantum fluctuations acting on the subsystem are *not* vanishing, and energy of the subsystem can be dissipated even at $T=0$. In particular, in clear contrast to the classical case, the coupling energy assumes quantum mechanically a *nonzero* value at *zero temperature*. This coupling energy then allows to rearrange energy and generates decoherence at $T=0$.

Second, the results for $\mathcal{F}$, $\mathcal{P}$, and $\mathcal{Q}$ always are located below a value of 0.999 85 for bit-flip errors and 0.975 for phase errors. This fact demonstrates that even smaller strengths of the coupling to the environment than the used $\gamma^x=10^{-6}$ or $\gamma^z=10^{-4}$ are necessary in order to obtain a desired value of 0.999 99 [11].

As discussed in the preceding section, set III should yield the best results since it requires the shortest operation time. However, as one observes in Fig. 3, this strongly depends on the operator mediating the coupling to the bath. For bit-flip error processes, it is the system operator

$$H_c^x=\frac{1}{2}(\sigma_1^x+\sigma_2^x)=\begin{pmatrix}0&1&1&0\\1&0&0&1\\1&0&0&1\\0&1&1&0\end{pmatrix}, \tag{5.1}$$

which couples to the bath. One readily observes that a long J pulse, during which the interqubit coupling operator

$$H_{12}=J\sigma_j^+\sigma_k^-=J\begin{pmatrix}0&0&0&0\\0&0&1&0\\0&1&0&0\\0&0&0&0\end{pmatrix} \tag{5.2}$$

is switched on, generates many transitions among different states. This can be seen by diagonalizing (the inner nonzero block of) H_{12} and by transforming H_c^x to the resulting eigenbasis of H_{12}. However, if the B_j^x fields are switched on, then not as many transitions occur. This can be seen by diagonalizing the corresponding system Hamiltonian $B^x\frac{1}{2}\sigma_j^x$ being switched on and by transforming H_c^x to the resulting eigenbasis. This explains why set I with a shorter J pulse yields better results than set II for the case of bit-flip errors, see Fig. 3(a).

For the case of phase errors, it is the system operator

$$H_c^z=\frac{1}{2}(\sigma_1^z+\sigma_2^z)=\begin{pmatrix}1&0&0&0\\0&0&0&0\\0&0&0&0\\0&0&0&-1\end{pmatrix}, \tag{5.3}$$

which couples to the bath. If now the B_j^x fields are switched on for a long time span, many transitions among different states are induced. In analogy to the previous case, H_c^z can be transformed to the eigenbasis of the corresponding system Hamiltonian $B^x\frac{1}{2}\sigma_j^x$ being switched on and the resulting operator has many nonzero matrix elements that generate many transitions. On the other hand, long J pulses are less effective since H_{12} and H_c^z commute. This explains why set III with shorter B_j^x pulses compared to set I yields better results. Put differently, a gate operation that takes longer than another may nevertheless perform better when subjected to an intermittently switched on system Hamiltonian, which is less sen-

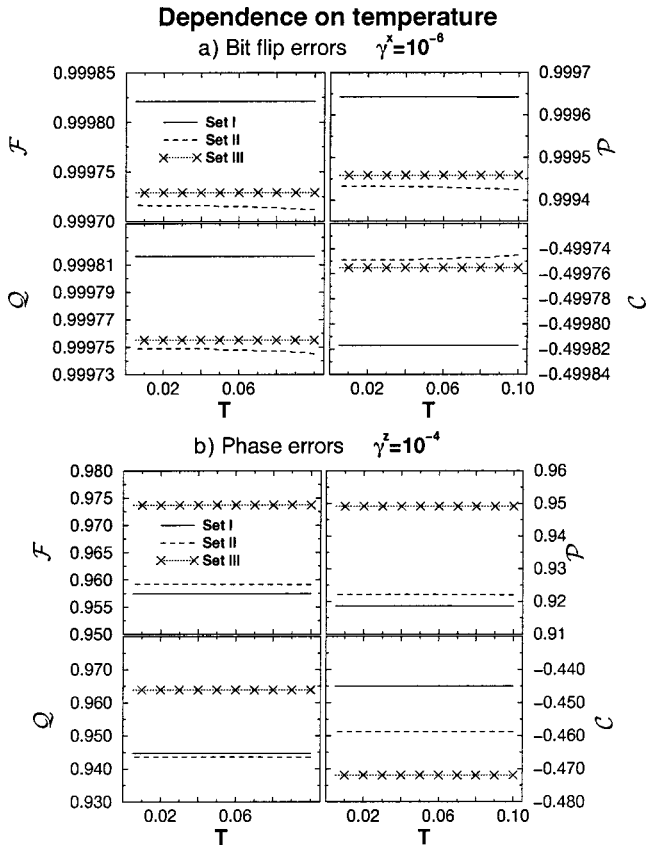

FIG. 3. Dependence of the fidelty $\mathcal{F}$, the purity $\mathcal{P}$, the quantum degree $\mathcal{Q}$, see Eqs. (4.1)–(4.3), and the entanglement capability $\mathcal{C}$ on temperature T for bit-flip errors (a) and phase errors (b). The temperature is scaled in units of $\hbar B^z/k_B$. The qubit parameters are given in Table I. The bath-interaction constant for the bit-flip errors is set at $\gamma^x=10^{-6}$ and for the phase errors at $\gamma^z=10^{-4}$.

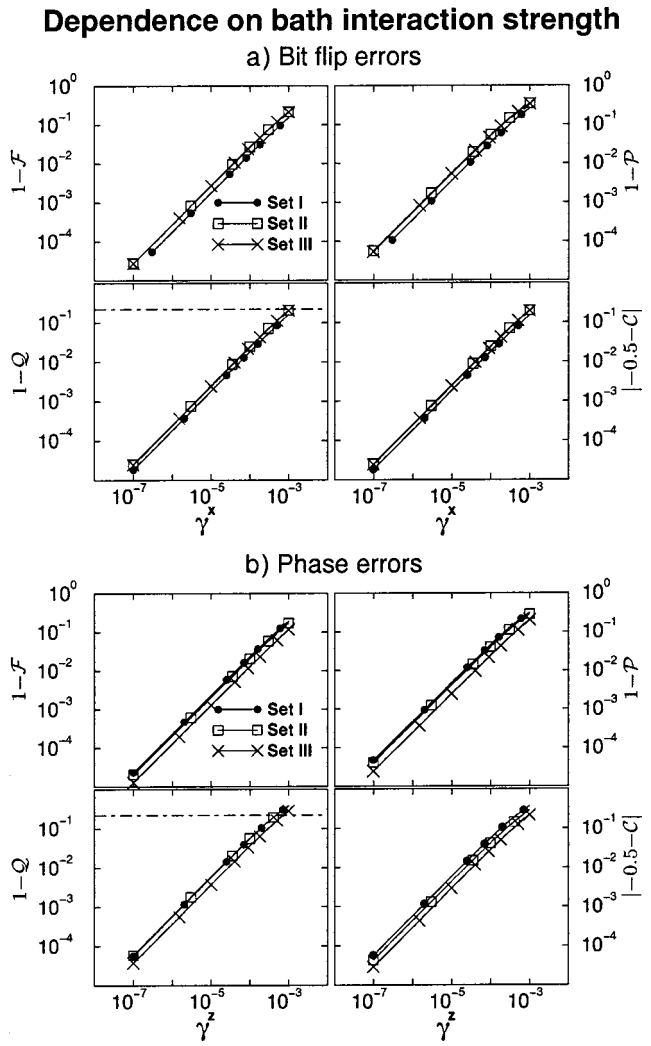

FIG. 4. Dependence of the four gate quantifiers on the dimensionless bath-interaction strength. Shown are the deviations from the ideal values, i.e., $1-\mathcal{F}$, $1-\mathcal{P}$, $1-\mathcal{Q}$, and $|-0.5-\mathcal{C}|$ in a log-log representation. Upper panel (a): bit-flip errors (γ^x); lower panel (b): phase errors (γ^z). The lower bound of $\mathcal{Q}\approx 0.78$ for the Clauser-Horne-Shimony-Holt inequality turns into an upper bound for the deviation $1-\mathcal{Q}$ and is indicated by the horizontal dotted-dashed line (see text). For the remaining parameters, see Table I.

sitive to decoherence. This qualitative conclusion is robust for the treatment of more realistic systems as they may arise in the future.

2. Dependence on the bath-interaction strength

As shown in the preceding section, the quality of the gate operation cannot be improved by lowering the temperature of the environment. The second possibility to reduce the influence of the environment is the shielding of the qubit system against external noise. This implies that the strengths of the bath interaction, $\gamma^{x/z}$, are reduced. The results for the dependence of the four gate quantifiers on the coupling constants $\gamma^{x/z}$ are depicted in Fig. 4.

One observes that the deviations of the four gate quantifiers from their ideal values depend linearly on the bath-interaction strengths. However, the prefactor is much larger than 1. Although one might have expected a linear increase of the deviations with increasing bath interaction in this small-damping regime, the deviations are *not* of the same order of magnitude as the bath-interaction strengths themselves but can be several orders of magnitude larger. This demonstrates that the bath-interaction strengths have to be less than 10^{-7} in order to achieve deviations being less than the desired 10^{-5} (see above). Moreover, the bath-interaction strengths have to be less than 10^{-3} in order to obtain values for the quantum degree larger than $\mathcal{Q}\approx 0.78$. Only then, the Clauser-Horne-Shimony-Holt inequality is violated and nonlocal correlations between the entangled qubits occur.

As in the previous section, we find again that the results for set I yield the best results when bit-flip errors are considered and set III performs best when phase errors are considered. The same argumentation as presented in Sec. V B 1 applies.

We note that although the individual results for the gate quantifiers appear to be similar, they contain different physical information. For instance, the purity $\mathcal{P}$ does not quantify the ''amount of entanglement'' between the two qubits, which, however, is characterized by the entanglement capability $\mathcal{C}$. In addition, one might also find different limits for

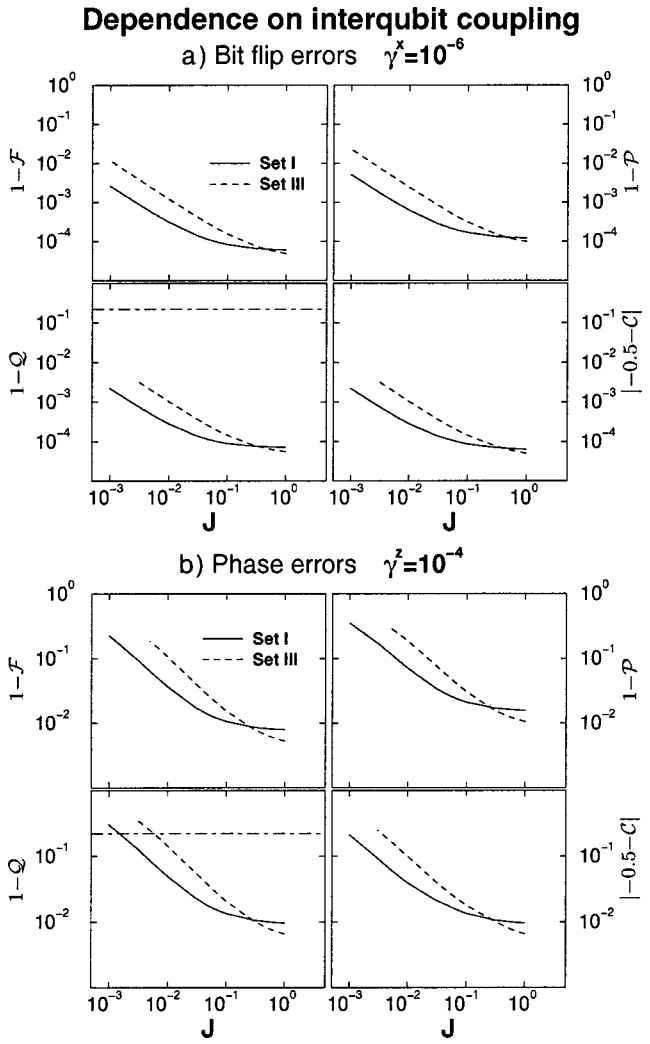

FIG. 5. Dependence of the gate quantifiers on the strength J of the interqubit coupling. Shown are the deviations from the ideal values, i.e., $1-\mathcal{F}$, $1-\mathcal{P}$, $1-\mathcal{Q}$, and $|-0.5-\mathcal{C}|$ in a log-log representation where J is scaled in units of B^z. Depicted are the results for parameter sets I and III from Table I. The upper panel (a) shows the results for the bit-flip error with $\gamma^x=10^{-6}$ while the lower panel (b) depicts the results for the phase error with $\gamma^z=10^{-4}$. The horizontal dot-dashed line marks the upper bound of $1-\mathcal{Q}\approx 0.22$ for the Clauser-Horne-Shimony-Holt inequality.

the quantifiers being required for a succesful *quantum* calculation.

3. Dependence on interqubit coupling strength

In the remaining part we address the dependence of the quality of the gate operation on the strength J of the interqubit coupling. Physically, one expects that an interqubit coupling strength J, which is comparable to the characteristic qubit energy B^z, i.e., $J\approx B^z$, would yield best performance results because of a corresponding minimal gate operation time. This is confirmed in Fig. 5 for the two different sets I and III (set II is equivalent to set I). Panel (a) illustrates the results for the bit-flip errors with $\gamma^x=10^{-6}$, and correspondingly panel (b) for the phase errors with $\gamma^z=10^{-4}$. For J approaching 1, the deviations of the quantifiers from their ideal values approach saturation values. Clearly, this ''minimal'' deviation cannot be avoided, since even in the fastest gate operation the influence of the bath is still present.

For set I, we find that for coupling strengths J smaller than 10^{-1} the deviations increase. For set III, however, the deviations increase already for larger values of J. Overall, we summarize this section by noting that the XOR gate operation deteriorates only weakly upon decreasing the interqubit coupling strength.

VI. CONCLUSIONS

In this work we have shown that the numerical quasiadiabatic-propagator path-integral method (QUAPI) of Makri and Makarov provides an appropriate method to investigate decohering quantum information processes that involve time-dependent Hamiltonians in presence of a coupling to an external environment. We have applied this iterative algorithm to the example of the quantum XOR gate operation and have obtained the full time-resolved evolution of the two-qubit system in presence of time-dependent external fields. No further approximations on the time evolution of the gate operation such as a Markovian evolution or extended time spans of the gate operation have been invoked.

We have investigated the quality of the quantum XOR operation by numerically determining four characteristic gate quantifiers, i.e., the fidelity $\mathcal{F}$, the purity $\mathcal{P}$, the quantum degree $\mathcal{Q}$, and the entanglement capability $\mathcal{C}$ of the gate. We have simulated the gate operation for three parameter sets. Thereby, we have suceeded in investigating systematically the quality of the gate operation as a function of the environmental temperature T, the bath-interaction strength γ, and the strength J of the interqubit coupling. Two different types of errors in the qubits have been modeled: (i) bit-flip errors and (ii) phase errors. We have elucidated how the different physical setups perform under these conditions. We have demonstrated that the quality of the gate operation does not only depend on the total operation time t_{XOR}. However, one has to carefully take into account the kind of the induced errors. In order words, this means that not always the shortest operation will yield the least deviations from the ideal operation. As another major finding we establish that the quality of the gate depends *only very weakly on temperature* but rather *strongly on the bath-interaction strength*. Although the deviations from the ideal case increase linearly with increasing bath-interaction strength, they can be several orders of magnitude larger than the bath-interaction strength itself. Moreover, we have illustrated that the interqubit coupling strength plays an important role and should not be smaller than $0.1E_0$ with E_0 being the typical energy scale of the qubit system. Since perfect switching mechanisms are assumed, these findings for the deviations from the ideal operation provide a lower bound since a real XOR gate operation may suffer from additonal errors induced by imperfect field pulses.

In order for a quantum information processor to operate optimally, the decoherent influence of the environment needs to be suppressed. Therefore, three different approaches are currently discussed: These are the techniques of quantum

error correction, fault tolerant quantum computation, and entanglement purification [26]. The general idea common to all three methods is to use for quantum information processing only a small subset of a larger set of entangled ancilla qubits. Although these ideas are very promising for small register lengths, the techniques become increasingly difficult if one attempts to realize large qubit registers in physical systems. Moreover, one has to keep track of the quantum state of the environment. Whilst these requirements are seemingly feasible for quantum optical information processing systems [38], they appear insufficient for condensed-matter systems with their characteristic huge number of environmental degrees of freedom.

An alternative approach consists in minimizing the occurrence of errors by *controlling decoherence* via the application of tailored time-dependent external fields to qubit systems [15,39–42]. For example, the application of a time-dependent periodic external field can induce a Floquet spectrum with degenerate quasienergy states [15,39,40] or it can move the qubit out off resonance with certain bath modes [42] thereby reducing decoherence. The suitability of such schemes to a quantum gate operation, however, remains to be demonstrated.

ACKNOWLEDGMENTS

We thank Milena Grifoni, Peter Talkner, Yuri Makhlin, and Robert Blick for helpful discussions. This work was supported by the Deutsche Forschungsgemeinschaft via Grant No. HA 1517/19-1 and by the Stichting voor Fundamenteel Onderzoek der Materie (M.T.).

[1] D. Deutsch, Proc. R. Soc. London, Ser. A **425**, 73 (1989); A. Barenco, *ibid.* **449**, 679 (1995); D. P. DiVincenzo, Phys. Rev. A **51**, 1015 (1995).

[2] S. Lloyd, Phys. Rev. Lett. **75**, 346 (1995); D. Deutsch, A. Barenco, and A. Ekert, Proc. R. Soc. London, Ser. A **449**, 669 (1995).

[3] V. Vedral, A. Barenco, and A. Ekert, Phys. Rev. A **54**, 147 (1996).

[4] P. W. Shor, in *Proceedings of the 35th Annual Symposium on Foundations of Computer Science*, edited by S. Goldwasser (IEEE Computer Society Press, Los Alamitos, CA, 1994); A. Ekert and R. Jozsa, Rev. Mod. Phys. **68**, 733 (1996).

[5] D. Deutsch, Proc. R. Soc. London, Ser. A **400**, 97 (1985).

[6] A. Barenco, Ch. H. Bennett, R. Cleve, D. P. DiVincenzo, N. Margolus, P. Shor, T. Sleator, J. A. Smolin, and H. Weinfurter, Phys. Rev. A **52**, 3457 (1995).

[7] W. G. Unruh, Phys. Rev. A **51**, 992 (1995).

[8] A. Garg, Phys. Rev. Lett. **77**, 964 (1996).

[9] G. Massimo Palma, K.-A. Suominen, and A. Ekert, Proc. R. Soc. London, Ser. A **452**, 567 (1996).

[10] R. Landauer, Proc. R. Soc. London, Ser. A **454**, 305 (1998).

[11] D. Loss and D. P. DiVincenzo, Phys. Rev. A **57**, 120 (1998).

[12] Yu. Makhlin, G. Schön, and A. Shnirman, Rev. Mod. Phys. **73**, 357 (2001).

[13] A. O. Caldeira and A. J. Leggett, Ann. Phys. (N.Y.) **149**, 374 (1983); **153**, 445(E) (1984); A. J. Leggett, S. Chakravarty, A. T. Dorsey, M. Fisher, A. Garg, and W. Zwerger, Rev. Mod. Phys. **59**, 1 (1987); **67**, 725(E) (1995).

[14] U. Weiss, *Quantum Dissipative Systems*, 2nd ed. (World Scientific, Singapore, 1999).

[15] M. Grifoni and P. Hänggi, Phys. Rep. **304**, 229 (1998).

[16] M. Grifoni, E. Paladino, and U. Weiss, Eur. Phys. J. B **10**, 719 (1999).

[17] M. Dubé and P. C. E. Stamp, Int. J. Mod. Phys. B **12**, 1191 (1998).

[18] M. Governale, M. Grifoni, and G. Schön, Chem. Phys. **268**, 273 (2001).

[19] D. Ahn, J. H. Oh, K. Kimm, and S. W. Hwang, Phys. Rev. A **61**, 052310 (2000).

[20] N. G. van Kampen, *Stochastic Processes in Physics and Chemistry* (North-Holland, Amsterdam, 1992).

[21] A. Suárez, R. Silbey, and I. Oppenheim, J. Chem. Phys. **97**, 5101 (1992).

[22] D. E. Makarov and N. Makri, Chem. Phys. Lett. **221**, 482 (1994); N. Makri and D. E. Makarov, J. Chem. Phys. **102**, 4600 (1995); **102**, 4611 (1995); N. Makri, J. Math. Phys. **36**, 2430 (1995).

[23] M. Thorwart and P. Jung, Phys. Rev. Lett. **78**, 2503 (1997); M. Thorwart, P. Reimann, P. Jung, and R. F. Fox, Chem. Phys. **235**, 61 (1998).

[24] M. Thorwart, P. Reimann, and P. Hänggi, Phys. Rev. E **62**, 5808 (2000).

[25] J. F. Poyatos, J. I. Cirac, and P. Zoller, Phys. Rev. Lett. **78**, 390 (1997).

[26] *The Physics of Quantum Information: Quantum Cryptography, Quantum Teleportation, Quantum Computation*, edited by D. Bouwmeester, A. Ekert, and A. Zeilinger (Berlin, Springer, 2000).

[27] J. E. Mooij, T. P. Orlando, L. Levitov, L. Tian, C. H. van der Wal, and S. Lloyd, Science **285**, 1036 (1999); T. P. Orlando, J. E. Mooij, L. Tian, C. H. van der Wal, L. Levitov, S. Lloyd, and J. J. Mazo, Phys. Rev. B **60**, 15 398 (1999); L. Tian, L. Levitov, C. H. van der Wal, J. E. Mooij, T. P. Orlando, S. Lloyd, C. J. P. M. Harmans, and J. Mazo, e-print cond-mat/99100062; C. H. van der Wal, A. C. ter Haar, F. K. Wilhelm, R. N. Schouten, C. J. P. M. Harmans, T. P. Orlando, S. Lloyd, and J. E. Mooij, Science **290**, 773 (2000); J. R. Friedman, V. Patel, W. Chen, S. K. Tolpygo, and J. E. Lukens, Nature (London) **406**, 43 (2000); G. Blatter, *ibid.* **406**, 25 (2000); L. B. Ioffe, V. B. Geshkenbein, M. V. Feigel'man, A. L. Fauchére, and G. Blatter, Nature (London) **398**, 679 (1999); G. Blatter, V. B. Geshkenbein, and L. B. Ioffe, e-print cond-mat/9912163.

[28] D. V. Averin, Solid State Commun. **105**, 659 (1998); Yu. Makhlin, G. Schön, and A. Shnirman, Nature (London) **398**, 305 (1999); V. Bouchiat, D. Vion, P. Joyez, D. Esteve, and M. Devoret, Phys. Scr. **T76**, 165 (1998); Y. Nakamura, Y. Pashkin, and J. Tsai, Nature (London) **398**, 786 (1999); D. Averin, *ibid.* **398**, 748 (1999).

[29] G. Burkard, D. Loss, and D. P. DiVincenzo, Phys. Rev. B **59**, 2070 (1999); A. Imamoğlu, D. D. Awschalom, G. Burkard, D. P. DiVincenzo, D. Loss, M. Sherwin, and A. Small, Phys. Rev. Lett. **83**, 4204 (1999); X. Hu and S. Das Sarma, Phys. Rev. A **61**, 062301 (2000); S. Bandyopadhyay, Phys. Rev. B **61**, 13 813 (2000);. J. Levy, e-print quant-ph/0101026.

[30] R. Blick and H. Lorenz, in *Proceedings of the IEEE International Symposium on Circuits and Systems, Geneva, Switzerland, 2000* (IEEE, Piscataway, 2000), pp. II245–II248; 1338.PDF on CD-ROM (ISBB 0-780-5485-0); A. W. Holleitner, C. R. Decker, K. Eberl, and R. H. Blick, e-print cond-mat/0011044; M. Bayer, P. Hawrylak, K. Hinzer, S. Fafard, M. Korkusinski, Z. R. Wasilewski, O. Stern, and A. Forchel, Science **291**, 451 (2001); J. H. Reina, L. Quiroga, and N. F. Johnson, *Proceedings of the ISI–Accademia dei Lincei Conference on Conventional and Non Conventional Computing (Quantum and DNA)* (Springer, Berlin, 2001).

[31] V. Privman, I. D. Vagner, and G. Kventsel, Phys. Lett. A **239**, 141 (1998); B. E. Kane, Nature (London) **393**, 133 (1998); D. P. DiVincenzo, *ibid.* **393**, 113 (1998); R. Vrijen, E. Yablonovitch, K. Wang, H. W. Jiang, A. Balandin, V. Roychowdhury, T. Mor, and D. DiVincenzo, Phys. Rev. A **62**, 012 306 (2000); D. Mozyrsky, V. Privman, and I. D. Vagner, Phys. Rev. B **63**, 085313 (2001).

[32] V. Privman, D. Mozyrsky, and I. D. Vagner, e-print cond-mat/0102308.

[33] R. Ionicioiu, G. Amaratunga, and F. Udrea, Int. J. Mod. Phys. B **15**, 125 (2001).

[34] R. P. Feynman and F. L. Vernon Jr., Ann. Phys. (N.Y.) **24**, 118 (1963).

[35] Ch. H. Bennett, G. Brassard, S. Popescu, B. Schumacher, J. A. Smolin, and W. K. Wootters, Phys. Rev. Lett. **76**, 722 (1996); J. F. Clauser, M. A. Horne, A. Shimony, and R. A. Holt, *ibid.* **23**, 880 (1969).

[36] A. Perea, Phys. Rev. Lett. **77**, 1413 (1996); M. Horodecki, P. Horodecki, and R. Horodecki, Phys. Lett. A **223**, 1 (1996).

[37] P. Mohanty, Physica B **280**, 446 (2000).

[38] C. J. Myatt, B. E. King, Q. A. Turchette, C. A. Sackett, D. Kielpinski, W. M. Itano, C. Monroe, and D. J. Wineland, Nature (London) **403**, 269 (2000); W. Schleich, *ibid.* **403**, 256 (2000).

[39] T. Dittrich, B. Oelschlägel, and P. Hänggi, Europhys. Lett. **22**, 5 (1993).

[40] P. Hänggi, in *Quantum Dynamics of Submicron Structures*, Vol. 29 of *NATO Advanced Studies Institute, Series E: Applied Sciences*, edited by H. A. Cerdeira, G. Schön, and B. Kramer (Kluwer, Boston, 1995).

[41] L. Viola, E. Knill, and S. Lloyd, Phys. Rev. Lett. **82**, 2417 (1999); L. Viola, S. Lloyd, and E. Knill, *ibid.* **83**, 4888 (1999).

[42] M. Thorwart, L. Hartmann, I. Goychuk, and P. Hänggi, J. Mod. Opt. **47**, 2905 (2000).